ORIGINAL ARTICLE
Iran J Allergy Asthma Immunol
In press.

MiR-425-5p Mediation of Malignant Behavior and Immune Escape of Cervical Cancer Cells by Targeting NCAM1

Mi Xiang[1], Yi Yu[1], Qin Gao[2], and Jie Xing[1]

[1] Department of Obstetrics, Puren Hospital Affiliated to Wuhan University of Science and Technology, Wuhan, China
[2] Department of Obstetrics and Gynecology, Puren Hospital Affiliated to Wuhan University of Science and Technology, Wuhan, China

Received: 8 January 2025; Received in revised form: 24 March 2025; Accepted: 19 April 2025

ABSTRACT

MicroRNA (miR)-425-5p is used as a molecular biomarker to identify cervical cancer (CxCa). However, few studies have examined the miR-425-5p-based modulation of the vital activities of CxCa cells.

The levels of neural cell adhesion molecule 1 (*NCAM1*) and miR-425-5p in CxCa tissues and cells were tested using western blot and reverse transcription quantitative polymerase chain reaction (RT-qPCR) tests. CxCa cells' malignant phenotype was examined through clone formation tests, and transwell tests. CD8+T cells were co-cultured with CxCa cells and then analyzed for apoptosis rates and the expression of activation proteins (granzyme B (GZMB) and perforin) as well as immune factors (tumor necrosis factor-alpha (TNF-α) and interferon-gamma (IFN-γ)) using flow cytometry, western blot, and enzyme-linked immunosorbent assay (ELISA) methods. Finally, in nude mouse experiments, the tumor size was measured for subcutaneous tumors, and the expression of CD8+T cell-related factors was detected.

The *NCAM1* and miR-425-5p were down-regulated and up-regulated in CxCa tissue and cells, respectively. After silencing miR-425-5p, CxCa cells showed attenuation in vitality, clone formation rate, and their capacities to migrate, penetrate, and evade immune responses. *NCAM1* was targeted and silenced by miR-425-5p. When *NCAM1* was silenced, it partially counteracted miR-425-5p's inhibitory effects on the immune escape and proliferation. In nude mice, the tumor size and weight decreased after silencing miR-425-5p, and levels of CD8, IFN-γ, TNF-α, perforin, and GZMB were elevated. However, these changes were reversed when *NCAM1* was silenced.

In conclusion, miR-425-5p mediates the biological behavior and immune evasion of CxCa cells by regulating *NCAM1*.

Keywords: MicroRNA-425-5p; Neural cell adhesion molecule 1; Tumor escape; Uterine cervical neoplasms

Corresponding Author: Jie Xing, MD;
Department of Obstetrics, Puren Hospital Affiliated to Wuhan University of Science and Technology, Wuhan, China. Tel: (+86 159) 7858 9898, Fax: (+98 027) 8636 2972, Email: fuweij8@163.com

INTRODUCTION

Cervical cancer (CxCa) ranks fourth among the most common carcinomas affecting women after breast, colorectal, and lung carcinomas.[1] Every year,

Published by Tehran University of Medical Sciences (http://ijaai.tums.ac.ir)

approximately 570,000 people worldwide are affected by CxCa, resulting in 310,000 deaths.[1–3] In countries with a high Human Development Index (HDI), 60 to 70% of patients with CxCa survive more than 5 years, while in countries with low HDI, the rate drops to less than 20%.[4,5] At present, the main options for treating CxCa are surgery, radiation, and chemotherapy. However, the effectiveness of treatment is contingent upon the stage of the disease. Treatment is difficult for those in advanced stages and usually involves a range of side effects, and the tumor can develop resistance.[6–8]

Immunotherapy, targeted therapy, and genetic approaches show promise for improving outcomes and survival in CxCa. However, these methods are still evolving, and many related studies are not comprehensive. It is important to find new molecular pathogenic pathways and cancer biomarkers for better control of CxCa.[9] The tumor microenvironment (TME) is a complex and delicate ecosystem composed of a variety of cell types, signaling molecules, and physical structures.[10] This environment provides the necessary conditions for tumor growth, invasion, and metastasis and also largely influences the tumor's response to treatment. Apoptosis and decreased activity of immune cells in the TME are the main mechanisms that lead to tumor immune escape,[11] which has been linked to CxCa metastasis and tumor invasion.[12]

$CD8^+$ T cells are the main anti-tumor immune effector cells *in vivo*. They can kill tumor cells and inhibit the invasion, metastasis and recurrence of tumors. If the activity of $CD8^+$ T cells is reduced or negated, tumor immune escape can occur more easily. However, it is not completely clear what mechanisms of immune escape are involved in the abnormal infiltration of immune $CD8^+$ T cells in the TME of CxCa. MicroRNA (miR) is involved in regulating cellular biological processes such as programmed death, immune modulation, inflammation, cell differentiation, and cell proliferation. Oncogenic or tumor-suppressive miR has been considered as biomarker candidates for identifying numerous cancers due to their varying expressions in tumor cells.[13] Furthermore, the augmentation or inhibition of miR expression has emerged as a novel strategy for disease treatment.[14]

MiR-425-5p is strongly associated with tumor genesis and expansion and exhibits increased expression in numerous tumor cells, which facilitates cancerous activities.[15–21] In tissues and cells that are affected by hepatocellular carcinoma, miR-425-5p levels are increased, resulting in a poorer prognosis for patients with this cancer and creating an environment conducive to the mobility and proliferation of cancer cells.[22] In tissues and cells affected by ovarian carcinoma, miR-425-5p levels are increased, but knocking down of this miR can prevent the cancer cells from invading, migrating, and multiplying.[23] MiR-425-5p levels are higher in CxCa cells, and decreasing its levels reduces the cell viability and induces apoptosis.[24,25] However, the role of miR-425-5p in the modulation of CxCa, particularly in relation to immune escape remains unclear. The aim of this work was to examine the impacts of miR-425-5p on immune escape and proliferation of CxCa cells and the underlying mechanisms.

MATERIALS AND METHODS

Clinical Samples

Samples of carcinoma tissues and para-carcinoma tissues were collected from 48 patients diagnosed with CxCa at Puren Hospital, affiliated with Wuhan University of Science and Technology. None of the patients had undergone preoperative radiotherapy or chemotherapy. This study followed the principles of the Declaration of Helsinki. All tests were conducted after obtaining informed consent from the participants and approval from the ethics committee of the hospital. Blood was also sampled from healthy female volunteers within the hospital and stored in heparin anticoagulant tubes at 4°C.

Cell Culture

Normal cervical epithelial cells (Ect1/E6E7) and CxCa cell lines (MS751, C-4I, C-33A, and HeLa) were obtained from the Cell Bank of the Chinese Academy of Sciences (Shanghai, China). All cells were cultivated in Roswell Park Memorial Institute (RPMI)-1640 medium (ORCPM0110B, ORiCells Biotechnology, Shanghai, China) with 10% fetal bovine serum (FBS). The cell culture incubator had saturated humidity with 5% CO_2 and a temperature of 37°C.

Cell Transfection

After a monolayer was formed and stuck to the well walls, the cells were sub-cultured, and then those entering the log phase were collected. Using Lipofectamine 3000 (L3000001, Invitrogen, Austin, TX, USA), the collected cells were transfected with

Published by Tehran University of Medical Sciences (http://ijaai.tums.ac.ir)

miR-425-5p inhibitor and its negative control (miR-425-5p inhibitor NC), as well as under-expressed neural cell adhesion molecule 1 (NCAM1) (shRNA-NCAM1) and its negative control (shRNA-NC). After transfection, the cells were cultured for an additional 48 hours prior to follow-up tests.

Cell Viability Test

Cell viability was tested using cell counting kit-8 (CCK-8) kits. The transfected CxCa cells were treated with trypsin, centrifuged, and resuspended in succession. Next, 1×10^4 cells were seeded into each well with 100 μL of culture medium. The plate was placed into an incubator (parameters: 37°C and 5% CO_2) for 48 hours. Subsequently, 10 μL of CCK-8 reagent (HY-K0301, MedChem Express, Monmouth Junction, NJ, USA) were dispensed into each well and mixed thoroughly, followed by another 2 hours of incubation. A microplate reader was then used to determine the optical density (OD) of the cells at 450 nm. Based on the results, the cells' survival rate was calculated as the percentage of the OD value of treated cells relative to that of untreated cells.

Clone Formation Test

Culture dishes containing 10 mL of culture medium were prepared, and groups of cells were seeded in them at a density of 100 cells per dish. The dishes were gently rotated to disperse the cells evenly and then placed in a cell incubator (parameters: 5% CO_2, 37℃) for 2 to 3 weeks of cell culture until visible clones appeared in the dishes. The dishes were then treated with 4% paraformaldehyde to fix the cell clones for 20 minutes.

After 2 washes with phosphate-buffered saline (PBS), the clones were stained for 30 minutes with an appropriate amount of Giemsa stain solution (C0133, Beyotime, Shanghai, China). After rinsing with PBS and air-drying, the cell clones were photographed using a microscope. The clone formation rate was calculated as the percentage of the number of cells clones relative to the number of seeded cells, and a cluster consisting of more than 50 cells was considered as one cell clone.

Transwell Cell Movement and Penetration Tests

The movement of cells was assessed using 8-μm transwells (Corning Incorporated, Corning, NY, USA), which were placed over a 24-well plate. Then, 100 μL of cell suspension with a cell density of 1×10^5/mL were added to each transwell. Below each transwell, 500 μL of RPMI-1640 medium supplemented with 10% FBS were dispensed. The plate was then put into an incubator (parameters: 5% CO_2, 37 ℃) for 24 hours of cell culture.

Next, the culture media in both the transwell and below it was discarded, and remaining cells were carefully wiped away with a cotton swab. The cells below the transwell (migrated cells) were fixed for 30 minutes in a solution containing 4% formaldehyde (P6148, Sigma, St Louis, MO, USA), followed by 30 minutes of staining in 0.1% crystal violet solution (C0121, Beyotime, Shanghai, China), followed by two rinses with PBS, and air drying. Lastly, the cells were observed and photographed using high-magnification microscopy, and the number of migrated cells was counted to determine their movement capacity. For penetration assessment of cells, 50 μL of Matrigel (354234, Corning Inc., Corning, NY, USA) were added to each transwell and air-dried at room temperature for 4 hours. Then, cell suspension and medium were injected into the transwells and lower compartments, followed by the same steps as in the movement assessment.

Flow Cytometry Tests

Flow cytometry was used to assess toxicity and apoptosis of CD8+T cells. Blood samples from healthy female volunteers were treated with gradient doses of Ficoll (Merck Millipore, Billerica, MA, the USA) and centrifuged to separate the peripheral blood mononuclear cells (PBMCs). The PBMCs were treated with human $CD8^+$T cell isolation kits (11348D, Invitrogen, Carlsbad, CA, USA) to isolate $CD8^+$T cells. The obtained $CD8^+$T cells were seeded in cell culture dishes at 1×10^6 cells/10 mL containing RPMI-1640 complete medium mixed with 10% FBS and 1% penicillin-streptomycin (15140122, Gibco, Grand Island, NY, USA).

Human CD3/CD28 T cell activator (11161D, Gibco, Grand Island, NY, USA) was added to the cell suspension at a ratio of 25 μL/10 mL, followed by 48 hours of culture at 37°C in 5% CO_2 and saturated humidity to stimulate the $CD8^+$T cells. The stimulated $CD8^+$T cells and transfected MS751 and HeLa cells were then co-cultured at a ratio of 10:1 for 16 hours. After co-culture, the instructions of PI/Annexin V-FITC cell stain kits (40302ES20, Yeasen Biotechnology, Shanghai, China) were followed to stain CxCa cells and $CD8^+$T cells. A NovoCyte Advanteon flow cytometer (Agilent Technologies, Santa Clara, CA, USA) was then

used to detect the staining, and the software FlowJo v10.6.2 (Tree Star, Ashland, OR, USA) was used for analysis. The results were used to assess the apoptosis rates of $CD8^+$T cells and $CD8^+$T cells.

Reverse Transcription Quantitative Polymerase Chain Reaction (RT-qPCR) Test

Tissues and cells were treated with Trizol reagent kits (DP424, TIANGEN, Beijing, China) to extract total RNA. The total RNA was reverse transcribed using prime script RT reagent kits (RR047A, Takara, Tokyo, Japan), and cDNA was synthesized. RT-qPCR tests were performed using the SYBR Green PCR kit (4309155, Applied Biosystems, DE, USA) and the ABI PRISM 7300 RT-PCR system (7300, ABI, Carlsbad, CA, USA). *GAPDH* and *U6* were used as internal controls for *NCAM1* and *miR-425-5p*, respectively, and their relative expression levels were calculated using the $2^{-\Delta\Delta Ct}$ method. The primers used are shown in Table 1.

Western Blot Test

Tissue or cell samples were immersed in lysis buffer (20101ES60, Yeasen Biotechnology, Shanghai, China) at 4°C for 30 minutes to extract proteins. An aliquot of 20 μg of protein sample was then isolated and subjected to 10% SDS-PAGE (sodium dodecyl sulfate-polyacrylamide gel electrophoresis) for protein separation. The separated proteins were transferred onto a polyvinylidene fluoride (PVDF) membrane, which was blocked in Tris-buffered saline with 0.2% Tween 20 (TBST) containing 5% non-fat milk for 1 hour at room temperature.

The membrane was rinsed and incubated overnight at 4°C with primary rabbit antibodies against NCAM1 (1:1000, ab237708, Abcam, Cambridge, UK), granzyme B (GZMB) (1:1000, ab255598, Abcam, Cambridge, UK), and perforin (1:1000, ab256453, Abcam, Cambridge, UK), as well as the internal control protein GAPDH (1:2500, ab9485, Abcam, Cambridge, UK). After incubation, the antibody solutions were discarded, and the membrane was rinsed with TBST. Subsequently, the membrane was incubated with goat anti-rabbit IgG secondry antibody (1:2000, ab6721, Abcam, Cambridge, UK) at 4°C for 30 minutes and then rinsed again with TBST. Enhanced chemiluminescence (ECL) reagent (P0018S, Beyotime, Shanghai, China) was applied for color development, and the membranes were imaged using a ChemiDoc Imaging System (5200, Tanon, Shanghai, China). The gray values of the protein bands were quantified using Image J 1.8.0 (National Institutes of Health, Bethesda, MD, the USA).

Bioinformatics Analysis

Kaplan–Meier survival curve analysis was conducted to examine the influence of miR-425-5p on the survival rate of patients with CxCa. The target gene of miR-425-5p was identified using TargetScan (http://www.targetscan.org/) and Gene Expression Profiling Interactive Analysis (GEPIA, http://gepia.cancer-pku.cn/). Gene-expression data from patients with CxCa were downloaded from the The Cancer Genome Atlas (TCGA) database (https://portal.gdc.cancer.gov/), and the expression of miR-425-5p was analyzed. The correlation between miR-425-5p and NCAM1 was assessed by Pearson correlation analysis.

Dual-luciferase Reporter Test

The 3'UTR of wild-type NCAM1 (NCAM1-WT) and mutant NCAM1 (NCAM1-MUT), which had bonded to the miR-425-5p sequence were cloned and inserted into dual-luciferase reporter vectors (E1330, Promega, Madison, WI, USA). Subsequently, Lipofectamine 3000 was added to CxCa cells to co-transfect them with both the NCAM1-WT and NCAM1-MUT recombinant plasmids, along with either a miR-425-5p inhibitor or miR-425-5p inhibitor NC separately. Transfection was allowed to proceed for 48 hours, after which the luciferase reporter gene activity in the transfected cells was measured using dual-luciferase reporter assay kits according to the manufacturer's instructions (RG027, Beyotime, Shanghai, China).

Nude Mice Test

Nude mice were subcutaneously injected with 100 μL of HeLa cells (1×10^6 cells/mice) to produce tumor xenografts. One week later, the 24 nude mice were split into 4 groups: the miR-425-5p inhibitor NC group, miR-425-5p inhibitor group, miR-425-5p inhibitor+shRNA-NC group, and miR-425-5p inhibitor+shRNA-NCAM1 group (each group n=6). The corresponding miR-425-5p inhibitor NC, miR-425-5p inhibitor, shRNA-NC, and shRNA-NCAM1 (10 μg) were injected every 3 days for 3 weeks after tumor formation. The tumor volume ($(length\times width^2)/2$) was measured weekly using a Vernier caliper. The transplanted tumor was removed, photographed, and weighed.

Immunohistochemistry Test

Fresh tumor tissue was fixed in paraformaldehyde, dehydrated with ethanol, embedded in paraffin, and cut into 4-μm-thick slices. The sections were cultured overnight with Ki-67 primary antibody (1:200, ab16667, Abcam, Cambridge, UK), followed by incubation, with secondary antibody (1:200, ab288151, Abcam, Cambridge, UK). All sections were observed under a microscope.

Immunofluorescence Test

The tumor sections were dewaxed, rehydrated into water, and antigen retrieval was performed using microwave heating. Sections were then blocked with 5% bovine serum albumin (BSA), and incubated at 37℃ for 1 hour. The serum was discarded, and primary antibody against CD8 (1:100, ab316778, Abcam, Cambridge, UK) was applied and left overnight at 4℃. Fluorescent secondary antibody (1:200, ab150077, Abcam, Cambridge, UK) was added and incubated for 60 min. After sealing with an anti-fade fluorescent quenching mounting medium, pictures were taken using a fluorescence microscope.

Enzyme-Linked Immunosorbent Assay (ELISA) for Assessing Immune Cytokines Secreted by CD8

Tumor tissue was obtained from the mice, homogenized, and then supernatant was collected. The supernatant was collected after co-culture, and an appropriate ELISA kit was used to detect the cytokine levels. ELISA kits for tumor necrosis factor-alpha (TNF-α, ab181421), interferon-gamma (IFN-γ, ab224197), and GZMB (ab238265) were obtained from Abcam (Cambridge, UK), and a perforin ELISA kit (21862) was purchased from MEIMIAN (Shuzhou, China).

Following the provided instructions, the co-cultured cell suspension was diluted, and 100 μL of the supernatant was added to an assay plate, followed by incubation at 37°C for 1.5 hours. Next, 100 μL of relevant antibodies were added to the plate, and the cells were incubated at 37°C for 1.5 hours, followed by administration of 100 μL of streptavidin-horseradish peroxidase conjugate (Streptavidin-HRP, S911, Invitrogen, Austin, TX, USA) for half an hour at the same temperature. The cells were then treated with 100 μL of color-developing agent and kept in the dark for 15 minutes, followed by the addition of 100 μL of stop solution to terminate the reaction. The OD values of the samples were measured at 450 nm using a microplate reader, and cytokine levels were calculated accordingly.

Data Processing

The data were analyzed using SPSS 26.0 (SPSS Inc., Chicago, IL, the USA) to vrify normal distribution and homogeneity of variance. Results are presented as the mean ± standard deviation. Two groups were compared using a *t*-test, while multiple groups were compared by one-way analysis of variance and Tukey's post hoc test. In all tests, statistical significance was denoted by *$p<0.05$, **$p<0.01$, and ***$p<0.001$.

RESULTS

Up-regulation of MiR-425-5p Level in CxCa Tissue and Adjacent Tissue

MiR-425-5p was significantly increased in CxCa tissues ($p<0.05$) (Figures 1A), and RT-qPCR tests were conducted to determine the effect of *miR-425-5p* on CxCa development. CxCa tissues had significantly higher *miR-425-5p* level than para-carcinoma tissues ($p<0.001$) (Figure 1B). The Kaplan–Meier survival analysis showed that poorer prognosis may be more likely for patients with CxCa who have high miR-425-5p levels ($p<0.01$) (Figure 1C). Moreover, compared to Ect1/E6E7 cells, the CxCa cell lines (MS751, C-4I, C-33A, and HeLa) exibited higher *miR-425-5p* levels, particularly MS751 and HeLa cells ($p<0.001$) (Figure 1D). MS751 and HeLa cells were selected for further experiments. Based on these findings, miR-425-5p may be a key factor in driving CxCa development.

Inhibition of CxCa Cell Growth, Movement, and Invasion by MiR-425-5p Suppression

MiR-425-5p inhibitor was administered to CxCa cells to reduce their levels of miR-425-5p and assess its influence on cell proliferation. The levels of *miR-425-5p* were significantly decreased in MS751 and HeLa cells ($p<0.01$) (Figure 2A). The outcomes of the CCK-8 assays and clone formation tests showed that these cells became less viable following the reduction of miR-425-5p level ($p<0.001$) (Figure 2B). Moreover, the number of MS751 and HeLa cell clones was reduced ($p<0.001$) (Figures 2C–D), which indicated that CxCa cell proliferation was inhibited. Additionally, transwell tests demonstrated a significant decrease in the number of migrating and invaded CxCa cells following miR-425-5p inhibition ($p<0.001$) (Figures 2E–H).

Published by Tehran University of Medical Sciences (http://ijaai.tums.ac.ir)

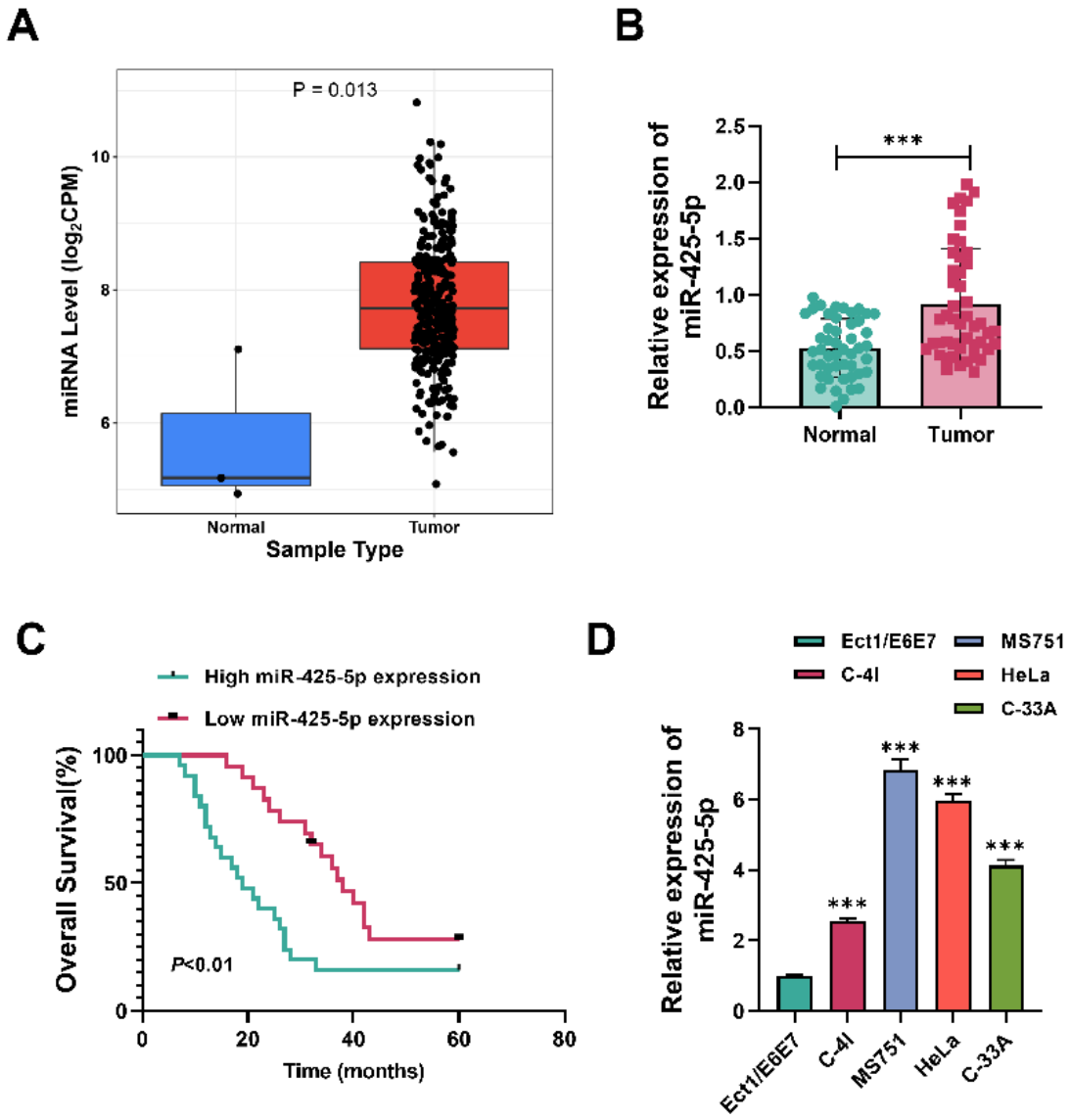

Figure 1. MicroRNA (miR)-425-5p level was up-regulated in cervical cancer (CxCa) tissue and adjacent tissue. A: miR-425-5p expression in CxCa tissues (n=48) in The Cancer Genome Atlas (TCGA) database, B: miR-425-5p expression in CxCa tissues (n=48) and para-carcinoma tissues, C: Survival curves for high and low expressions of miR-425-5p, D: miR-425-5p contents in Ect1/E6E7 cell and MS751/C-4I/C-33A/HeLa cells.

Published by Tehran University of Medical Sciences (http://ijaai.tums.ac.ir)

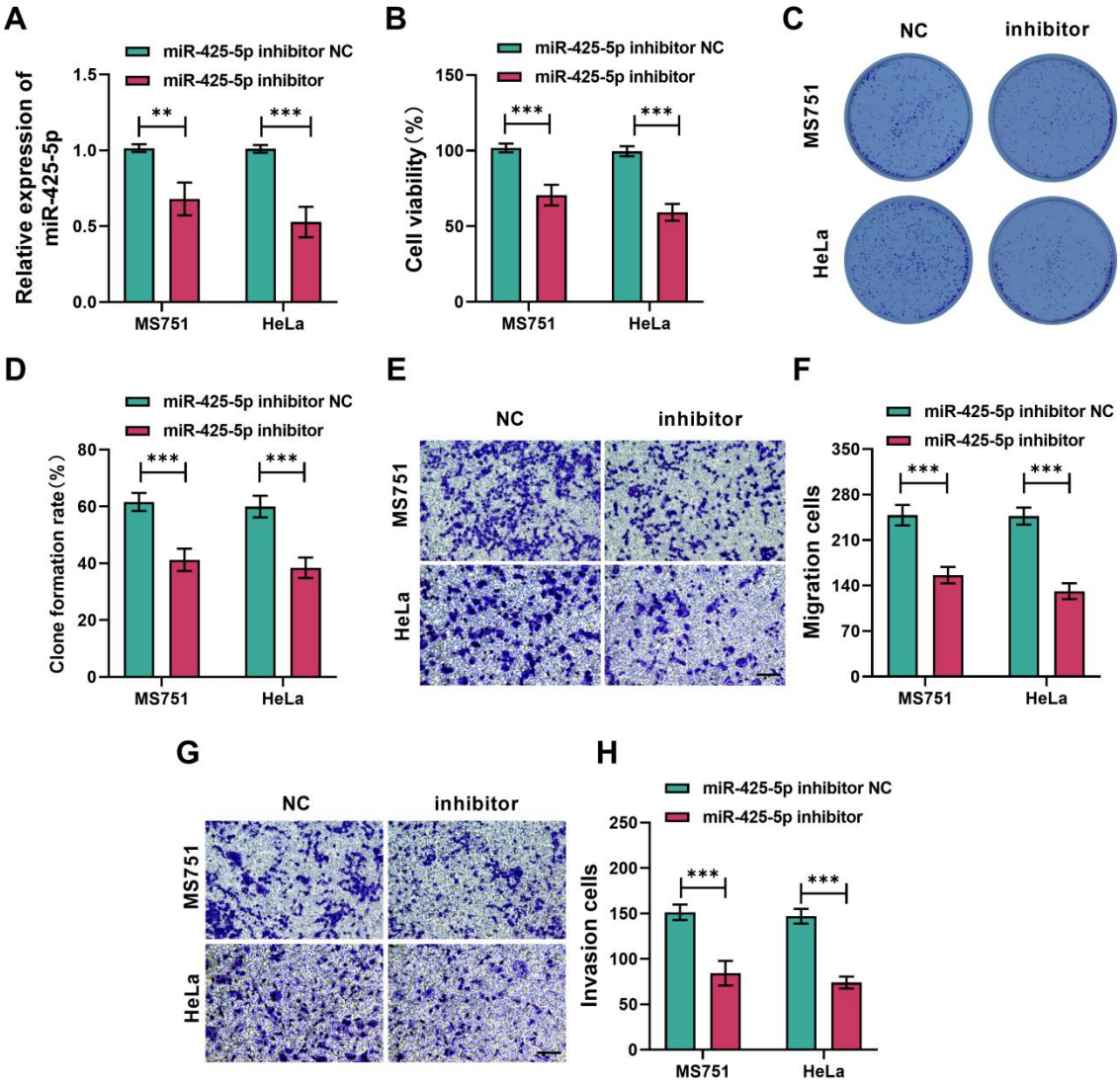

Figure 2. MicroRNA (miR)-425-5p suppression inhibits cervical cancer (CxCa) cell growth, migration and invasion. A: Relative levels of miR-425-5p, B: Cell viability after miR-425-5p was suppressed, C-D: Clone formation assays, E-F: Transwell migration assays showing cell movement capacity (×20, 100 µm), G-H: Transwell invation assays demonstrating cell invation capacity (×20, 100 µm)

Inhibition of CxCa Cells' Immune Escape by MiR-425-5p Knockdown

The impact of low miR-425-5p level with the immune escape of CxCa cells was assessed. MS751 and HeLa cells with reduced miR-425-5p expression were separately co-cultured with $CD8^{+}$T cells. The FCM analysis revealed an increase in the proportion of apoptotic CxCa cells, indicating enhanced cytotoxicity of CD8+ T cells (Figure 3A), while the apoptosis rate of $CD8^{+}$T cells decreased (p<0.001) (Figure 3B).

Following the knockdown of miR-425-5p, there was a marked elevation in the protein levels of GZMB and perforin—key molecules involved in CD8+ T cell activation, as evidenced by Western blot analysis (p<0.001) (Figure 3C). Additionally, ELISA results demonstrated an increase in the secretion of immune cytokines TNF-α and IFN-γ by CD8+ T cells (p<0.001) (Figure 3D). These findings suggest that silencing miR-425-5p enhances the immune-mediated killing capacity of CD8+ T cells, thereby reducing their immune escape.

Published by Tehran University of Medical Sciences (http://ijaai.tums.ac.ir)

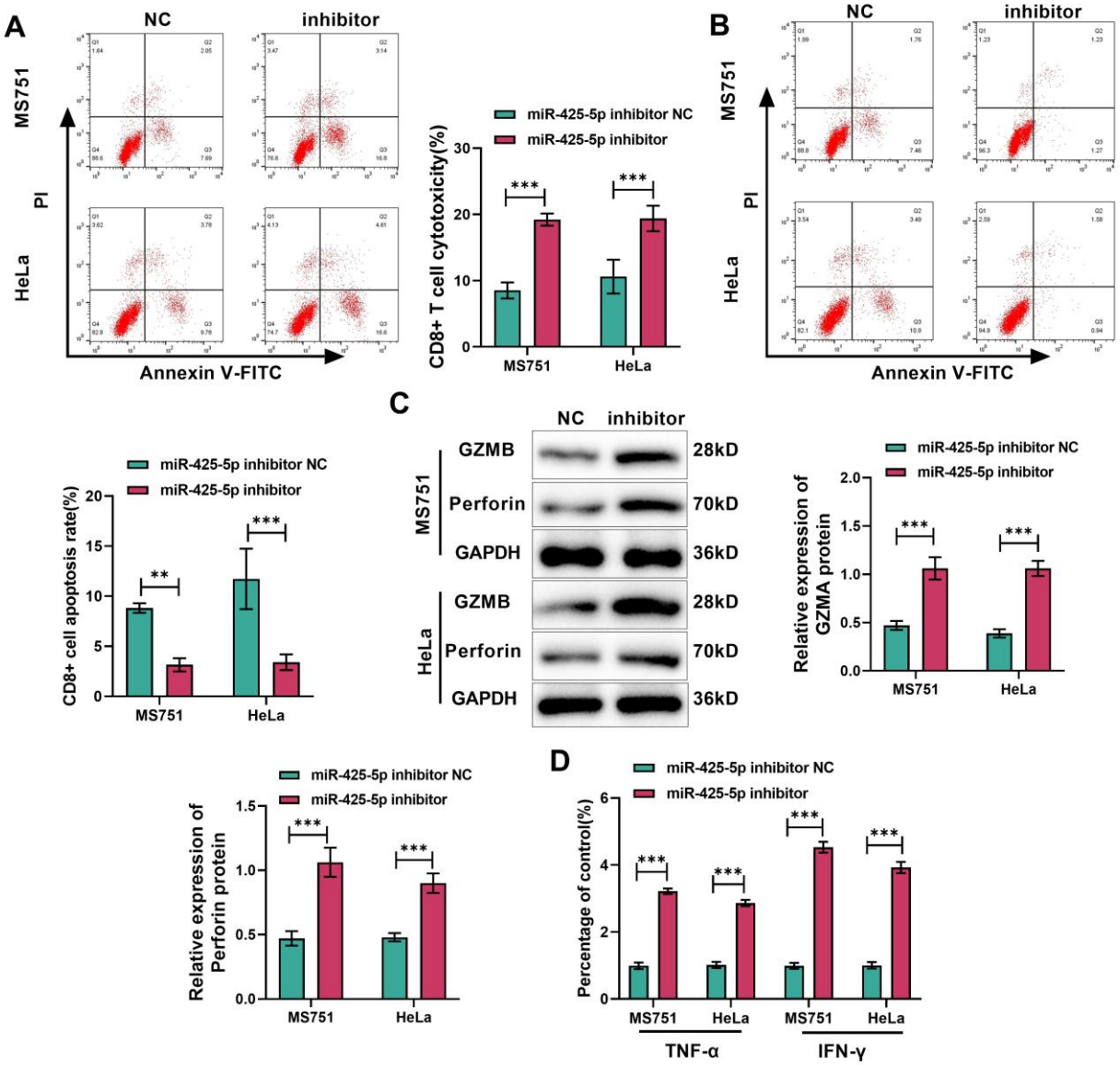

Figure 3. MicroRNA (miR)-425-5p knockdown restrained immune escape of cervical cancer (CxCa) cells. A: Consequences of flow cytometry tests on CD8$^+$ T cells' toxicity, B: Consequences of flow cytometry tests on CD8$^+$ T cells' apoptosis, C: Consequences of western blot tests on granzyme B (GZMB) and Perforin, D: Consequences of enzyme-linked immunosorbent assay (ELISA) tests on the relative expressions of interferon-gamma (IFN-γ) and tumor necrosis factor-alpha (TNF-α) secreted by CD8 cells

MiR-425-5p Targeting of NCAM1

Using prediction online tools Tar getScan and GEPIA, phospholamban (*PLN*) and *NCAM1* were screened out as the target genes of miR-425-5p. Analysis of the TCGA CESC database revealed that NCAM1 expression was significantly decreased in CxCa tissues compared to normal tissues (Figure 4A). According to western blot analysis, the NCAM1 expression in CxCa cells with low miR-425-5p level was higher than the PLN protein expression (p<0.01) (Figures 4B, C). Thus, *NCAM1* was confirmed as miR-425-5p's major regulatory gene, and their binding sites illustrated in Figure 4D.

Dual-luciferase reporter assays demonstrated that the miR-425-5p inhibitor significantly attenuated the luciferase activity of NCAM1-WT construct, but had no effect on the NCAM1-MUT construct (p<0.01) (Figures 4E, F). This further confirmed that that miR-425-5p directly targets NCAM1. Subsequent assessments of NCAM1 expression in CxCa tissues and cell lines showed significant down-regulation in both protein and mRNA levels of NCAM1 in CxCa cells and tissues (MS751, C-4I, C-33A, and HeLa) compared to normal tissues and Ect1/E6E7 cells (p<0.001) (Figures 4G–J). Furthermore, Pearson correlation analysis demonstrated a negative association between miR-425-5p and NCAM1expression levels (Figure 4K). In summary, these results support that miR-425-5p negatively regulates NCAM1 by direct targeting.

NCAM1 Knockdown and CxCa Cell Growth, Movement, and Invasion

Knockdown of NCAM1 partially rescued the inhibitory effects of miR-425-5p knockdown on CxCa cell proliferation, migration, and invasion. Following transfection with shRNA against NCAM1, Western blot analysis confirmed a marked reduction in NCAM1 protein levels in MS751 and HeLa cells (p<0.05) (Figures 5A, B). Furthermore, transfection of miR-425-5p inhibitors decreased miR-425-5p levels and prevent CxCa cells from suppressing immune responses and cell proliferation. To explore the role of NCAM1 further, co-transfection of shRNA-NCAM1 was performed to downregulate NCAM1 expression in cells with inhibited miR-425-5p.CxCa cells with down-regulation of both miR-425-5p and NCAM1exibited significantly higher cell viability and clone formation rates compared to cells with only miR-425-5p inhibition (p<0.01) (Figures 5C–E).

Similarly, migration and invasion assays showed that the enhanced motility and invasive capacity induced by miR-425-5p inhibition were partially reversed by NCAM1 silencing (p<0.001) (Figures 5F–I). These findings indicate that the effects of miR-425-5p inhibition on cell proliferation, migration, and invasion are, at least in part, mediated through NCAM1.

NCAM1 Knockdown and Immune Escape by CxCa Cells

Knockdown of NCAM1 partially rescued the inhibitory effect of miR-425-5p knockdown on immune escape by CxCa cells. In the flow cytometry analysis, the apoptosis rate of CxCa cells was significantly reduced, and $CD8^{+}$T cell toxicity was markedly decreased (p<0.001) (Figures 6A, B), while the apoptosis rate of CD8+ T cells increased with NCAM1 downregulation (p<0.001) (Figures 6C, D). Additionally, levels of GZMB and perforin were decreased (p<0.01) (Figures 6E–G), as well as TNF-α and IFN-γ (p<0.01) (Figures 6H, I). These observations suggest that down-regulating NCAM1 attenuates the enhancement of CD8+ T cell responses mediated by the miR-425-5p inhibitor. It implies that miR-425-5p may regulate critical functions of CxCa cells such as proliferation and immune escape by targeting NCAM1.

CxCa Cell Tumorigenicity and Immune Escape *In Vivo*

Down-regulation of miR-425-5p reduced CxCa cells' tumorigenicity and immune escape *in vivo.* The tumors size and weight were significantly reduced following miR-425-5p knockdown and markedly increased after NCAM1 knockdown (p<0.001) (Figures 7A–C). The expression trend of Ki-67 was consistent with the tumor size, which decreased after miR-425-5p knockdown and increased after NCAM1 knockdown (p<0.001) (Figures 7D, E). These findings suggest that silencing miR-425-5p inhibits the tumorigenic capacity of HeLa cells.

Simultaneously, immunofluorescence and ELISA analyses revealed that levels of CD8, IFN-γ, TNF-α, perforin, and GZMB in tumor tissues were significantly increased after miR-425-5p knockdown and significantly decreased after NCAM1 knockdown (p<0.05) (Figures 7F–I). These results further demonstrate that silencing miR-425-5p suppresses CxCa immune escape *in vivo*. Combined with in vitro experiments, the results indicate that silencing miR-425-5p inhibits CxCa's malignant behavior and immune escape through up-regulating NCAM1.

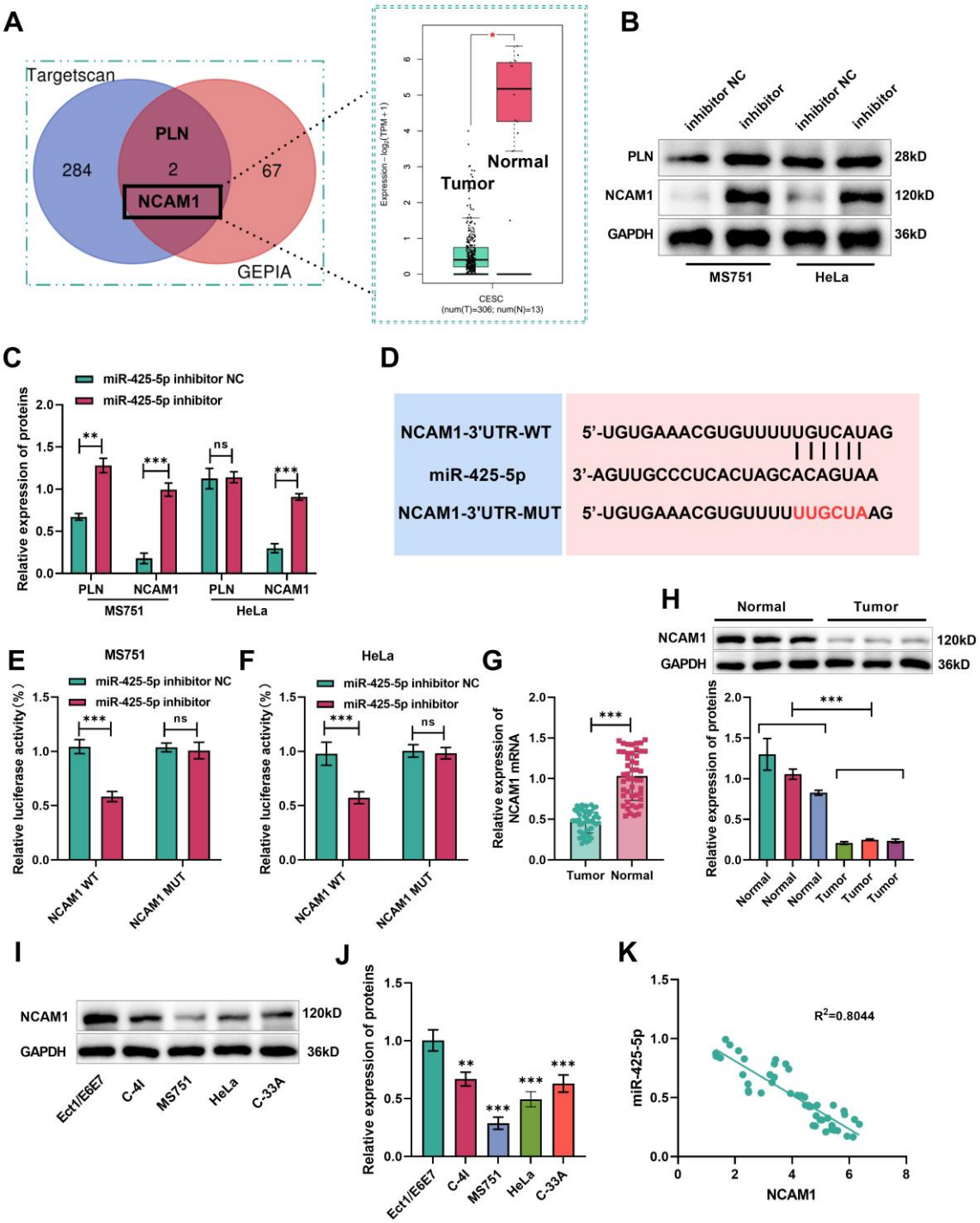

Figure 4. MicroRNA (miR)-425-5p targeted neural cell adhesion molecule 1 (NCAM1). A: Screening of target genes phospholamban (PLN) and NCAM1 from Target Scan and Gene Expression Profiling Interactive Analysis (GEPIA) databases, along with the relative expressions of NCAM1 in carcinoma tissues and para-carcinoma tissues in the GEPIA database, B-C: Selection of target genes PLN and NCAM1, D: Pairing of miR-425-5p with the wild and mutant genes, E-F: Dual-luciferase activity, G-J: NCAM1 level in cancer tissue and cancer cell, respectively, K: Correlation analysis between miR-425-5p and NCAM1

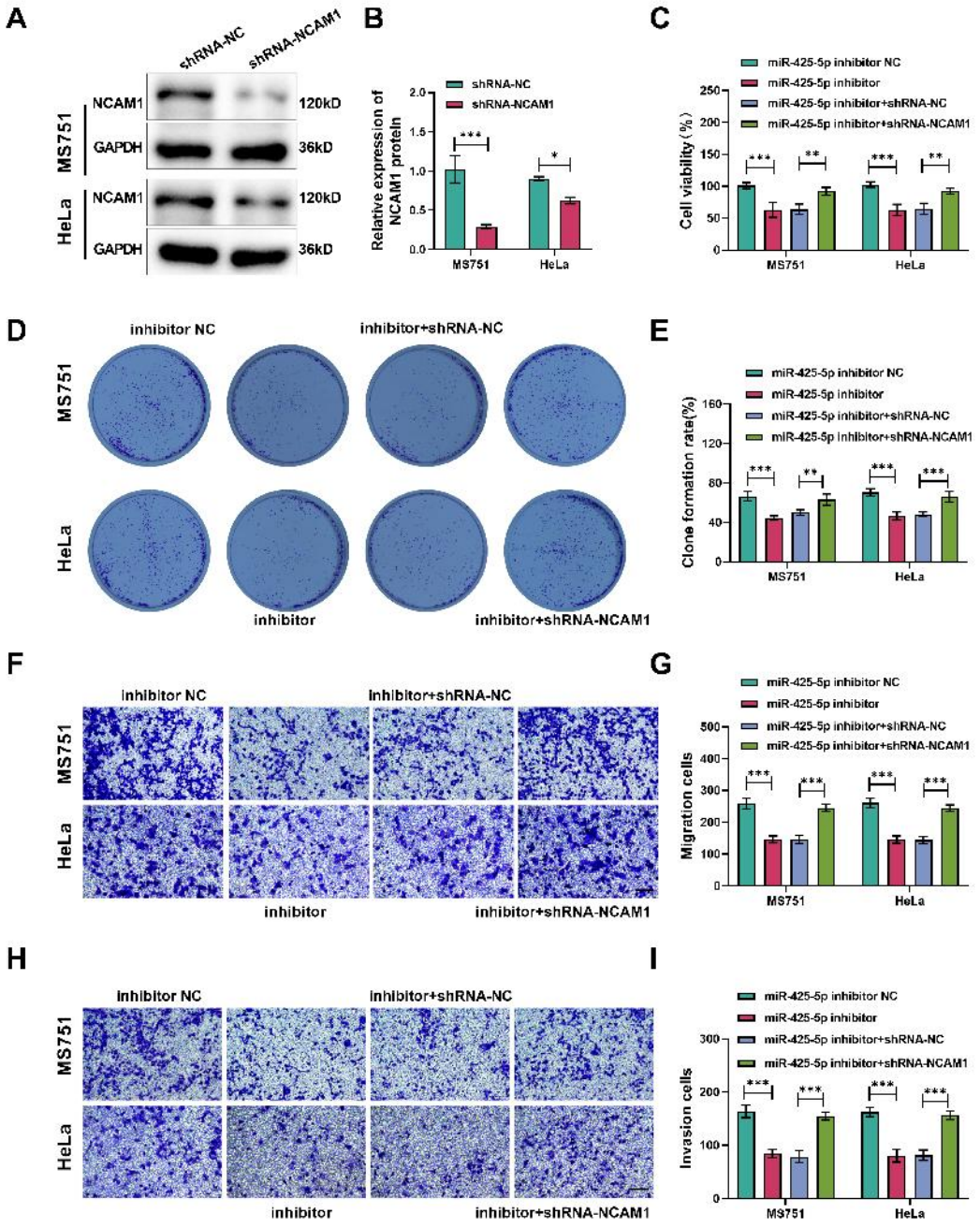

Figure 5. Knockdown of neural cell adhesion molecule 1 (NCAM1) partially rescued the inhibitory effect of MicroRNA (miR)-425-5p knockdown on cervical cancer (CxCa) cell proliferation, migration and invasion. A-B: NCAM1 relative level in cells after transfection, C: The impact of NCAM1 on cell viability, D-E: Cell cloning and visualization analysis, F-G: Transwell-based test on cell movement (×20, 100 µm), H-I: Transwell-based test on cell penetration (×20, 100 µm).

Published by Tehran University of Medical Sciences (http://ijaai.tums.ac.ir)

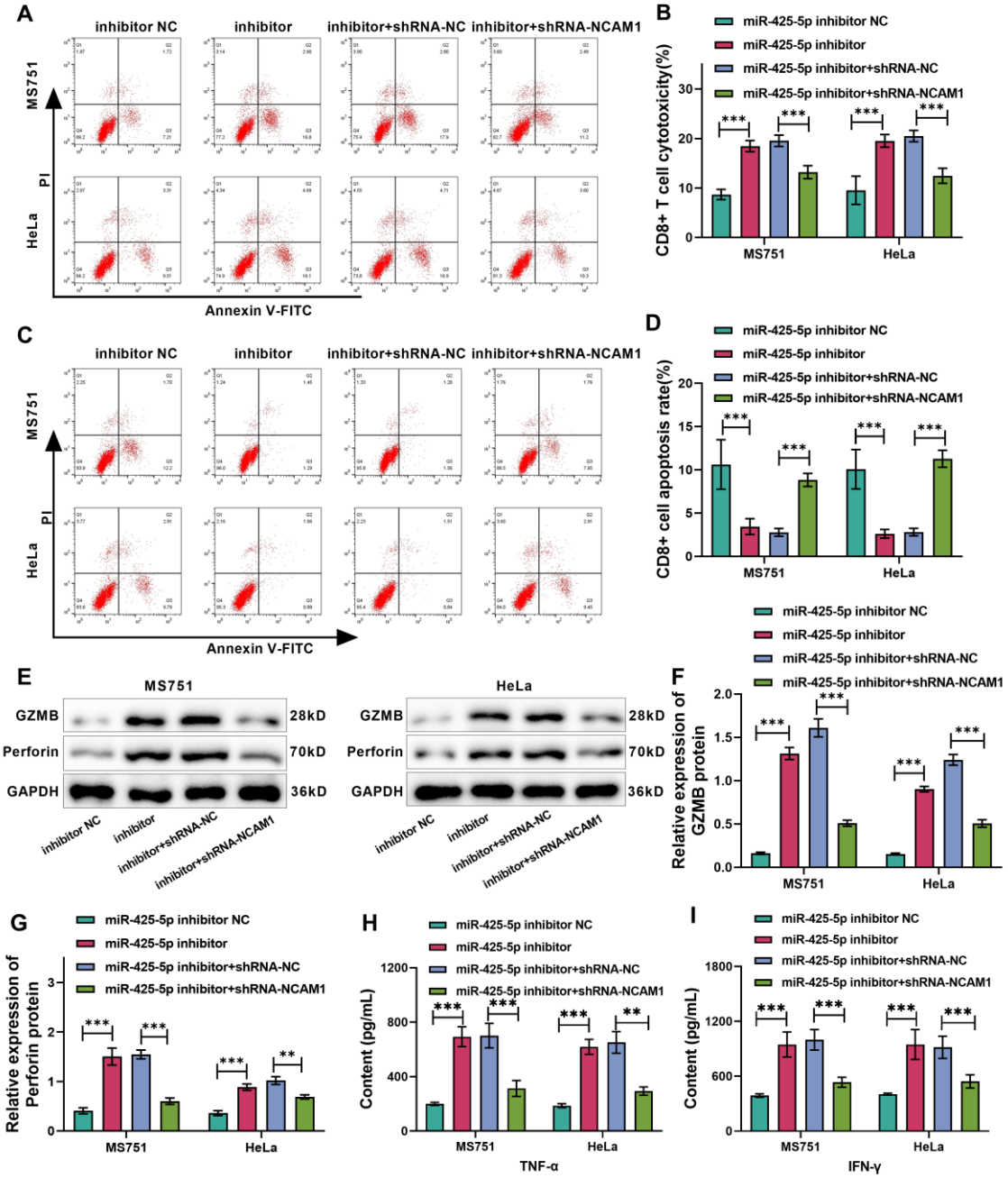

Figure 6. Knockdown of neural cell adhesion molecule 1 (NCAM1) partially rescued the inhibitory effect of MicroRNA (miR)-425-5p knockdown on immune escape of cervical cancer (CxCa) cells. A-B: Consequences of flow cytometry tests on $CD8^+$ T cells' toxicity, C-D: Consequences of flow cytometry tests on $CD8^+$ T cells' apoptosis, E-G: Consequences of western blot tests on granzyme B (GZMB) and Perforin, H-I: Consequences of enzyme-linked immunosorbent assay (ELISA) tests on the relative expressions of interferon-gamma (IFN-γ) and tumor necrosis factor-alpha (TNF-α) secreted by CD8 cells.

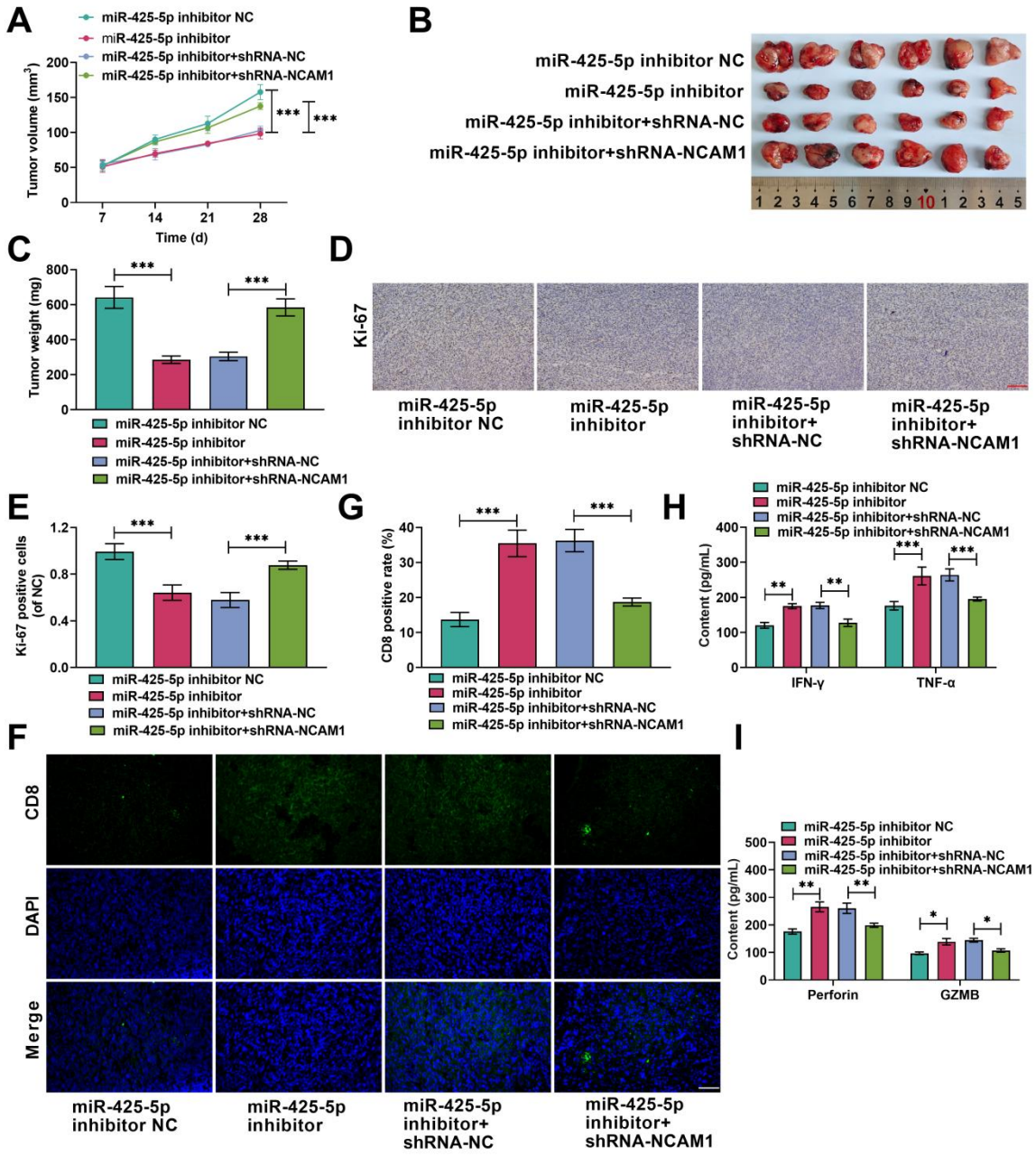

Figure 7. Down-regulation of MicroRNA (miR)-425-5p restrained cervical cancer (CxCa) cell tumorigenicity and immune escape *in vivo*. A: The size of subcutaneous tumor, B-C: On the 28 th day, the tumor mass was weighed, D-E: Consequences of immunohistochemistry tests on Ki-67 level (×20, 100 µm), F-G: Consequences of immunofluorescence tests on CD8 level (×40, 50 µm), H-I: Consequences of enzyme-linked immunosorbent assay (ELISA) kit tests on interferon-gamma (IFN-γ), tumor necrosis factor-alpha (TNF-α), Perforin and granzyme B (GZMB) levels.

Published by Tehran University of Medical Sciences (http://ijaai.tums.ac.ir)

DISCUSSION

High-risk human papillomavirus (HPV) triggers the onset of CxCa. HPV can lead to precancerous lesions of normal cervical epithelium.[26] CxCa can be treated surgically in the early stages, but not in advanced stages or after metastasis.[27] Therefore, it is important to find biomarkers and molecular targets that can accurately predict CxCa is crucial to facilitate the development of diagnostic and therapeutic strategies.

Aberrant expression of miR can interfere with CxCa evolution by regulating its target gene.[28–30] MiR-425-5p and NCAM1 were respectively up-regulated and down-regulated in CxCa cells. MiR-425-5p targets NCAM1 exerting a negative regulatory effect. Silencing NCAM1 was shown to partially mitigate the effects of miR-425-5p inhibition on CxCa cell proliferation and immune escape. Thus, the NCAM1/miR-425-5p pathway could be a plausible route in the development of CxCa.

Also recognized as CD56, NCAM1 belongs to the immunoglobulin superfamily and function as a cell adhesion protein.[31] It participates in the processes of cell adhesion and growth and is linked to the occurrence, development, and prognosis of various tumors.[32–34] As a surface marker on natural killer (NK) cells, NCAM1 can influence the development, maturation, and movement of immune cells and their process of killing target cells.[35]

NK cells and NKT cells are major immune cells with NCAM1 expression. They can generate cytotoxicity and induce apoptosis of target cells, as well as release cytokines to regulate immune balance and the activities of dendritic cells and T cells.[36–38] The present results revealed that after the silencing of NCAM1, there was enhancement of CxCa cells' migration, proliferation, and invasive capacities, while increasing apoptosis of CD8+ T cells and decreasing their cytotoxicity. These results suggest that NCAM1 participates in modulating CxCa cells' malignant behavior and immune escape, which hinders cancer progression.

$CD8^+$T cells are a primary factor in inhibiting tumor cells immune responses. The persistence of their cytotoxic function determines their level of anti-tumor immune response.[39] $CD8^+$T cells are cytotoxic and have large amounts of GZMB and perforin. The GZMB enzyme that cleaves and activates caspases and is delivered into cancer cells by perforin, where it cleaves substrates such as caspase-3, leading to cell apoptosis.[40,41] Additionally, $CD8^+$T cells can also secrete TNF-α, IFN-γ, and other cytokines, which are associated with immune functions and inflammatory processes.[42–44]

Within the tumor microenvironment (TME),, the metabolism of $CD8^+$T cells can often weaken the anti-tumor immune response, and tumor cells evade immune surveillance.[45] $CD8^+$T cells compete with tumor cells for nutrients within the TME, consuming glutamine and glucose and releasing immunosuppressive substances and ions, including potassium, lactic acid, and urea. Other immune cells like regulatory T cells and tumor-related macrophages also produce factors that suppress CD8+ T cell function.[46–48]

In co-culture experiments, CxCa cells with low miR-425-5p levels demonstrated increased apoptosis, while the apoptosis rate of $CD8^+$T cells decreased. The culture supernatant showed elevated GZMB and perforin expression, along with TNF-α and IFN-γ. *In vivo*, CD8, IFN-γ, TNF-α, perforin, and GZMB increased in tumor tissues after miR-425-5p silencing. These changes indicated that a low miR-425-5p level is conducive to the anti-tumor immune responses of $CD8^+$T cells, impeding $CD8^+$T cell metabolism within the TME.

Conversely, downregulation of NCAM1 yielded opposite outcomes, likely because miR-425-5p under-expression leads to the up-regulating NCAM1. Hence, the outcomes were opposite to those obtained with shRNA-NCAM1. In addition, tumor-associated macrophages (TAMs) and regulatory T cells (Treg) are also main types of immunosuppressive cells in the TME and have key roles in tumor immune escape. We speculate that miR-425-5p may inhibit immune escape by regulating TAM polarization or local clearance of Treg, and then affecting CxCa, which will be the consider for further investigation.

This study primarily explored the effects of miR-425-5p's on CxCa-cell immune escape and proliferation, as well as its potential pathways of action. However, *in vitro* results require further verification through *in vivo* and in clinical trials. This study also had limitations because many genes and proteins play a role in tumors and the immune system, but nude mice lack immune cells. Therefore, nude mice cannot accurately simulate the immune attack of the body's immune system on tumors. In addition, this study mainly focused on MS751 and HeLa cells, and further studies are needed to explore the effect of miR-425-5p on other CxCa cells and clarify how miR-425-5p regulates CxCa by targeting NCAM1.

MiR-425-5p holds a prominent place in the proliferastion and immune escape of CxCa cells by

targeting NCAM1. The miR-425-5p/NCAM1 axis may serve as a potential target for CxCa treatment. Such findings may help develop new therapeutic drugs and targeted therapies for CxCa. However, further work is needed to unravel miR-425-5p's effects in vivo, develop targeted drugs for inhibiting miR-425-5p, or directly knocking out miR-425-5p through CRISPR/Cas9. Nanocarriers (such as liposomes, polymer nanoparticles) could also be used to improve the targeting of miR-425-5p and NCAM1, and clinical toxicity trials are needed to test such drugs. Such drugs could also be used together with chemotherapy, other targeted drugs, and immunotherapy to improve the clinical response of patients with CxCa. Future studies should also integrate pathological research, genetic mutations, and immunological characteristics to achieve personalized precision treatment.

STATEMENT OF ETHICS

All tests for this survey were receiving approval from the Ethics Committee of Puren Hospital Affiliated to Wuhan University of Science and Technology (No.2024976).

FUNDING

Not applicable.

CONFLICT OF INTEREST

The authors declare no conflicts of interest.

ACKNOWLEDGMENTS

Not applicable.

DATA AVAILABILITY

The data supporting the findings of this study can be obtained from the corresponding author, upon request.

AI ASSISTANCE DISCLOSURE

No applicable.

REFERENCES

1. Sung H, Ferlay J, Siegel RL, Laversanne M, Soerjomataram I, Jemal A, et al. Global Cancer Statistics 2020: GLOBOCAN Estimates of Incidence and Mortality Worldwide for 36 Cancers in 185 Countries. CA Cancer J Clin. 2021;71(3):209–49.
2. Ashrafizadeh M. Cell Death Mechanisms in Human Cancers: Molecular Pathways, Therapy Resistance and Therapeutic Perspective. J Cancer Biomol Ther. 2024;1(1):17–40.
3. McCluggage WG, Singh N, Gilks CB. Key changes to the World Health Organization (WHO) classification of female genital tumours introduced in the 5th edition (2020). Histopathology. 2022;80(5):762–78.
4. Forman D, de Martel C, Lacey CJ, Soerjomataram I, Lortet‐Tieulent J, Bruni L, et al. Global burden of human papillomavirus and related diseases. Vaccine. 2012;30(Suppl 5):F12‐23.
5. Wakeham K, Kavanagh K. The burden of HPV-associated anogenital cancers. Curr Oncol Rep. 2014;16(9):402.
6. Ferrall L, Lin KY, Roden RBS, Hung CF, Wu TC. Cervical Cancer Immunotherapy: Facts and Hopes. Clin Cancer Res. 2021;27(18):4953–73.
7. Gottesman MM, Fojo T, Bates SE. Multidrug resistance in cancer: role of ATP-dependent transporters. Nat Rev Cancer. 2002;2(1):48–58.
8. Wang K, Tepper JE. Radiation therapy-associated toxicity: Etiology, management, and prevention. CA Cancer J Clin. 2021;71(6):437–54.
9. Burmeister CA, Khan S, Czerniecki BJ, Erbeck K, Gawlik C, Jones HL, et al. Cervical cancer therapies: Current challenges and future perspectives. Tumour Virus Res. 2022;13:200-38.
10. Aftab M, Purohit H, Jain V, Bhowmick S, Verma RS. Urine miRNA signature as a potential non-invasive diagnostic and prognostic biomarker in cervical cancer. Sci Rep. 2021;11(1):10323.
11. Rupaimoole R, Slack FJ. MicroRNA therapeutics: towards a new era for the management of cancer and other diseases. Nat Rev Drug Discov. 2017;16(3):203–22.
12. Liu D, Zhang H, Cui M, Chen C, Feng Y. Hsa-miR-425-5p promotes tumor growth and metastasis by activating the CTNND1-mediated beta-catenin pathway and EMT in colorectal cancer. Cell Cycle. 2020;19(15):1917–27.
13. Liu S, Wang Q, Liu Y, Xia ZY. miR-425-5p suppresses tumorigenesis and DDP resistance in human-prostate cancer by targeting GSK3beta and inactivating the Wnt/beta-catenin signaling pathway. J Biosci. 2019;44.

14. Wu S, Mo Y, Peng M, Yang J, Tang T, Long Y, et al. Downregulation of ZC3H13 by miR-362-3p/miR-425-5p is associated with a poor prognosis and adverse outcomes in hepatocellular carcinoma. Aging (Albany NY). 2022;14(5):2304–19.
15. Xiao S, Zhu H, Luo J, Wu Z, Xie M. miR-425-5p is associated with poor prognosis in patients with breast cancer and promotes cancer cell progression by targeting PTEN. Oncol Rep. 2019;42(6):2550–60.
16. Yuan Z, Liu C, Wang L, Xie Q, Chen Y, Zheng X, et al. Long noncoding RNA LINC-PINT regulates laryngeal carcinoma cell stemness and chemoresistance through miR-425-5p/PTCH1/SHH axis. J Cell Physiol. 2019;234(12):23111–22.
17. Zhang Z, Zhang Y, Liu Y, Su J, Xie B. Clinical value of miR-425-5p detection and its association with cell proliferation and apoptosis of gastric cancer. Pathol Res Pract. 2017;213(8):929–37.
18. Zhao Y, Liu H, Sun Y, Zhang N, Ji S, Liu C, et al. LncRNA-MSC-AS1 inhibits the ovarian cancer progression by targeting miR-425-5p. J Ovarian Res. 2021;14(1):109.
19. Rao D, Guan S, Huang J, Chang Q, Duan S. miR-425-5p Acts as a Molecular Marker and Promoted Proliferation, Migration by Targeting RNF11 in Hepatocellular Carcinoma. Biomed Res Int. 2020;2020:6530973.
20. Wu Z, Liu W, Jiang X, Wang Y, Guo L, Li G, et al. MiR-425-5p accelerated the proliferation, migration, and invasion of ovarian cancer cells via targeting AFF4. J Ovarian Res. 2021;14(1):138.
21. Nascimento NPG, Gally TB, Borges GF, Campos LCG, Kaneto CM. Systematic review of circulating MICRORNAS as biomarkers of cervical carcinogenesis. BMC Cancer. 2022;22(1):862.
22. Zhang Y, Xu X, Ge R, Zhou Y, Ye M, Sun X. Downregulation of microRNA-425-5p suppresses cervical cancer tumorigenesis by targeting AIFM1. Exp Ther Med. 2019;17(6):4032–8.
23. Richart RM. A modified terminology for cervical intraepithelial neoplasia. Obstet Gynecol. 1990;75(1):131–3.
24. Uyar D, Rader J. Genomics of cervical cancer and the role of human papillomavirus pathobiology. Clin Chem. 2014;60(1):144–6.
25. Deng B, Qu L, Li J, Liu F, Tang Q, Yang Y, et al. MicroRNA-142-3p inhibits cell proliferation and invasion of cervical cancer cells by targeting FZD7. Tumour Biol. 2015;36(11):8065–73.
26. Kogo R, Mimori K, Tanaka F, Komune S, Mori M. The microRNA-218\~Survivin axis regulates migration, invasion, and lymph node metastasis in cervical cancer. Oncotarget. 2015;6(2):1090–100.
27. Shen S, Zhang S, Liu P, Wang J, Du H. Potential role of microRNAs in the treatment and diagnosis of cervical cancer. Cancer Genet. 2020;248–249:25–30.
28. Guan G, Zhang X, Liu H, Wang H, Wang Z. Upregulation of Neural Cell Adhesion Molecule 1 (NCAM1) by hsa-miR-141-3p Suppresses Ameloblastoma Cell Migration. Med Sci Monit. 2020;26\:e923491.
29. Kim HS, Kim S, Kim E, Lee H, Yang W, Lee YJ, et al. Directly reprogrammed natural killer cells for cancer immunotherapy. Nat Biomed Eng. 2021;5(12):1360–76.
30. Kriegsmann K, Warth A, Muley T, Harms A, Herpel E, Winter H, et al. Role of Synaptophysin, Chromogranin and CD56 in adenocarcinoma and squamous cell carcinoma of the lung lacking morphological features of neuroendocrine differentiation: a retrospective large-scale study on 1170 tissue samples. BMC Cancer. 2021;21(1):486.
31. Zhang Y, Wang X, Xu B, Ma X, Wang Y, Zhang R, et al. Baseline immunity and impact of chemotherapy on immune microenvironment in cervical cancer. Br J Cancer. 2021;124(3):414–24.
32. Gunesch JT, Dixon KO, Rahman R, Al-Attar A, Skov J, Lauron EJ, et al. CD56 regulates human NK cell cytotoxicity through Pyk2. Elife. 2020;9:e57346.
33. Van Acker HH, Capsomidis A, Smits EL, Van Tendeloo VF. CD56 in the Immune System: More Than a Marker for Cytotoxicity? Front Immunol. 2017;8:892.
34. Vayrynen JP, Vornanen JO, Sajanti SA, Böhm JP, Tuomisto A, Mäkinen MJ. Spatial Organization and Prognostic Significance of NK and NKT-like Cells via Multimarker Analysis of the Colorectal Cancer Microenvironment. Cancer Immunol Res. 2022;10(2):215–27.
35. Weber B, Bornhöfft D, Fölster-Holst R, Geisel J, Sterry W, Worm M. Distinct interferon-gamma and interleukin-9 expression in cutaneous and oral lichen planus. J Eur Acad Dermatol Venereol. 2017;31(5):880–6.
36. Fu C, Jiang A. Dendritic Cells and CD8 T Cell Immunity in Tumor Microenvironment. Front Immunol. 2018;9:3059.
37. Liu X, Zhang Z, Ruan J, Pan Y, Magupalli VG, Wu H, et al. Inflammasome-activated gasdermin D causes pyroptosis by forming membrane pores. Nature. 2016;535(7610):153–8.

38. Ramljak D, Pirš M, Seme K, Debeljak Z, Avčin T, Ihan A. Early Response of CD8+ T Cells in COVID-19 Patients. J Pers Med. 2021;11(3):221.
39. Corridoni D, Antanaviciute A, Gupta T, Ortiz-Muñoz G, Franzè E, Povey E, et al. Single-cell atlas of colonic CD8(+) T cells in ulcerative colitis. Nat Med. 2020;26(9):1480–90.
40. Kumar J, Kim K, Lee SH, Park S, Kim D, Han J, et al. Deletion of Cbl-b inhibits CD8(+) T-cell exhaustion and promotes CAR T-cell function. J Immunother Cancer. 2021;9(1):e001647.
41. Tang M, Tian L, Luo G, Yu X. Interferon-Gamma-Mediated Osteoimmunology. Front Immunol. 2018;9:1508.
42. Zheng Y, Wang X, Huang M. Metabolic Regulation of CD8(+) T Cells: From Mechanism to Therapy. Antioxid Redox Signal. 2022;37(17–18):1234–52.
43. Chang CH, Qiu J, O'Sullivan D, Buck MD, Noguchi T, Curtis JD, et al. Metabolic Competition in the Tumor Microenvironment Is a Driver of Cancer Progression. Cell. 2015;162(6):1229–41.
44. Ho PC, Bihuniak JD, Macintyre AN, Staron M, Liu X, Amezquita R, et al. Phosphoenolpyruvate Is a Metabolic Checkpoint of Anti-tumor T Cell Responses. Cell. 2015;162(6):1217–28.
45. Ottensmeier CH, Perry KL, Harden EL, Stasakova J, Jenei V, Fleming J, et al. Upregulated Glucose Metabolism Correlates Inversely with CD8+ T-cell Infiltration and Survival in Squamous Cell Carcinoma. Cancer Res. 2016;76(14):4136–48.
46. Chang CH, Qiu J, O'Sullivan D, Buck MD, Noguchi T, Curtis JD, et al. Metabolic Competition in the Tumor Microenvironment Is a Driver of Cancer Progression. Cell. 2015;162(6):1229-41.
47. Ho PC, Bihuniak JD, Macintyre AN, Staron M, Liu X, Amezquita R, et al. Phosphoenolpyruvate Is a Metabolic Checkpoint of Anti-tumor T Cell Responses. Cell. 2015;162(6):1217-28.
48. Ottensmeier CH, Perry KL, Harden EL, Stasakova J, Jenei V, Fleming J, et al. Upregulated Glucose Metabolism Correlates Inversely with CD8+ T-cell Infiltration and Survival in Squamous Cell Carcinoma. Cancer research. 2016;76(14):4136-48.